

An Adaptive Gradient Regularization Method

Huixiu Jiang¹, Ling Yang², Yu Bao³, and Rutong Si^{4*}

¹Department of Computer Science, Illinois Institute of Technology Chicago, USA

²School of Computer Science, Peking University, China

³Bioinformatics Center, Institute for Chemical Research, Kyoto University, Japan

⁴The Abdus Salam International Centre for Theoretical Physics, Strada Costiera 11, Trieste 34151, Italy

hjiang34@hawk.iit.edu, yangling0818@163.com, bitdanger51@gmail.com, rsi@ictp.it

Abstract

Optimizer plays an important role in neural network training with high efficiency and performance. Weight update based on its gradient is the central part of the optimizer. It has been shown that normalization and standardization operation on weight and gradient can accelerate the training process and improve performance such as Weight Standardization (WS), weight normalization (WN) and gradient normalization (GN); there is also gradient centralization (GC). In this work, we introduce a new optimization technique based on the gradient magnitude in a gradient vector named adaptive gradient regularization (AGR), which normalizes the gradient vector in all dimensions as a coefficient vector and subtracts the product of the gradient and its coefficient vector by the vanilla gradient. It can be viewed as an adaptive gradient clipping method. We show that the AGR can improve the loss function Lipschitzness with a more stable training process and better generalization performance. AGR is very simple to be embedded into vanilla optimizers such as Adam and AdamW with only three lines of code. Our experiments are conducted in image generation, image classification and language representation, which shows that our AGR improves the training result. We have released our code in <https://github.com/hjiang24/AGR-method/tree/master>

1. Introduction

Deep learning has achieved great success in broad fields, e.g., vision tasks (Guo et al. 2022), natural language processing (Goldberg 2016), and recommendation system (Zhang et al. 2019b). Apart from the increasing development of large datasets (Yu et al. 2015) and abundant computing resources, e.g., GPUs and TPUs, elegant neural network architectures (Liu et al. 2017) and optimization algorithms (Ghadimi and Lan 2013) are also the key ingredients in deep learning. For optimization algorithms, stochastic gradient-based algorithms contribute to the success of deep learning on large-scale datasets with satisfactory speed and local minimum loss.

There are a variety of stochastic gradient-based algorithms, among which SGD (Ruder 2016; Bottou 2012) is the earliest and most representative algorithm for its simplicity and efficiency in many sophisticated network

architectures. Subsequently, many variants of SGD have been proposed for faster training speed and better prediction accuracy, e.g. SGD with momentum (SGDM) (Qian 1999), Adam (Kingma and Ba 2014), AdamW (Loshchilov and Hutter 2017), Adagrad (Duchi et al. 2011), RMSProp (Zou et al. 2019) and ACProp (Zhuang et al. 2021). The introduction of first-order momentum and second-order momentum combined with adaptive learning strategy make them popular in current deep neural networks (DNNs) training.

There are some techniques to improve training stability. The most prevalent method is normalization, e.g., batch normalization (BN) (Ioffe and Szegedy 2015), group normalization (GN) (Wu and He 2018), layer normalization (LN) (Ba et al. 2016), and instance normalization (IN) (Ulyanov et al. 2016). The design on sample/feature, weight, and weight gradient are useful and general optimization techniques on DNN training, which is to find a satisfactory solution in weight space with speed. BN utilizes statistics of samples in a mini-batch to approximate statistics of entire training sets to solve the internal covariate shift problem. Hence, training speed has been improved significantly under the same accuracy with much higher learning rates and less care about initialization.

Many Network architectures have incorporated BN as the indispensable layer, and the ideology it invents provides insights for subsequent research. Weight Normalization (WN) (Salimans and Kingma 2016) inspired by BN decouples the length of weight vectors from their direction, which is simple and provides much of the speed-up of full batch normalization. Weight Standardization (WS) (Qiao et al. 2019) applies zero mean and unit variance on the weights to smooth the loss landscape by reducing the Lipschitz constants of the loss and the gradients. Inspired by WN and WS, gradient centralization (GC) (Yong et al. 2020a) is proposed to operate on the gradients of weight by simply centralizing the gradient vectors to have zero mean, which could regularize both the weight space and output feature space to boost the generalization performance of DNNs.

Inspired by the research mentioned above, we propose a new optimization technique to operate on weight gradients by Hadamard product with learnable coefficients instead of the zero-mean standardization of weight gradients, which is simple and could also be a kind of adaptive gradient

*Corresponding author

Copyright © 2025, Association for the Advancement of Artificial Intelligence (www.aaai.org). All rights reserved.

regularization (AGR). The main contributions of our work are as follows:

- We propose a new optimizer technique, named Adaptive Gradient Regularization (AGR), which could not only smooth the training loss but also have better generalization performance in multiple network architectures on different tasks, e.g., image generation, image classification, and token prediction.
- We analyze the theoretical foundation of AGR and find it operates a new regularization method on gradients and provides a direction in the weight iteration process, which is also viewed as a new adaptive learning rate scaling method.

2. Related work

Weight: Weight Normalization (WN) (Salimans and Kingma 2016; Gitman and Ginsburg 2017) is a simple reparameterization of the weight vectors in DNNs that accelerates the convergence of SGD optimization, which is an alternative to Batch Normalization (BN). Weight Standardization (WS) (Qiao et al. 2019) is targeted at the micro-batch training where the small batch sizes are not enough for training DNNs with Batch Normalization (BN), which normalizes weight vectors instead of features like Batch Normalization and can smooth the loss landscape by reducing the Lipschitz constants of the loss and the gradients.

Gradient: Gradient is calculated for loss back-propagation in deep network training to update weight. Various gradient improvement methods have been proposed for a more stable training process and better generalization performance. Momentum is defined as the first-order momentum and the second-order momentum of gradients to be introduced as optimizer development method (Qian 1999; Botev et al. 2017). In SGDM, momentum helps SGD accelerate in the relevant direction and dampen oscillations by considering the previous updates (Ruder 2016). SGD with Nesterov Acceleration (Nesterov 2014; Tran et al. 2022) takes into account the momentum term in the calculation of the gradient, by considering the future position of the parameter. Gradient clipping (Zhang et al. 2019a; Chen et al. 2020; Menon et al. 2019) and gradient normalization (Wu et al. 2021) were proposed for training convergence acceleration. Gradient clipping is to solve the gradient exploding problem by scaling the gradient to keep it small when the gradient becomes too large, improving training stability and accelerating convergence. gradient normalization is similar to weight normalization decoupling the length of gradients from their direction. Gradient Centralization (GC) (Yong et al. 2020b) centralizes gradients to have zero means, which can be viewed as a projected gradient descent method with a constrained loss function and regularizes the weight space and output feature space boosting the generalized performance of DNNs.

Distinguished from weights and activations, the distribution of gradients is approximately lognormal(Chmiel et al. 2020; Guo et al. 2021). The distribution has a few gradients

with huge magnitude and many gradients with small magnitude. The logarithmic scale of such distribution is close to a symmetric normal (Gaussian) distribution around the mean as zero, which is consistent with the assumption that gradient in the neural network is sampled from Gaussian distribution (Wiedemann et al. 2020). During the training process, the gradient distribution should be maintained as unchanged as possible. In other words, the difference between gradients needs to be as small as possible. That is why gradient clipping was proposed to accelerate DNN training. However, the current gradient modification methods could not adjust each gradient according to its magnitude dynamically. It is not challenging to set an appropriate threshold in gradient clipping.

Adaptive learning rate: Determining a good learning rate can prevent the system from diverging in terms of the loss function and slow learning (Chen et al. 2018a). Adagrad (Duchi et al. 2011) scales the learning rate adaptively in each iteration for all dimensions based on the sum of the outer product of the gradients, considering all previous updates. However, the learning rate will be almost unchanged if the gradient is large at the beginning and small subsequently. RMSprop (Zou et al. 2019) introduces decay factors in the outer product of the gradients instead of simple summing of them, solving the problem of Adagrad. Adam (Kingma and Ba 2014) and AdamW (Loshchilov and Hutter 2017) also adapt the ideology to scale the learning rate adaptively. Adam (Xie et al. 2022) is an adaptive Nesterov algorithm reformulating the vanilla Nesterov momentum to develop a new Nesterov momentum estimation (NME), which improves the model training speed across multiple networks.

3 Adaptive Gradient Regularization

3.1 Motivation

Normalization and standardization have been applied to features and weight vectors, respectively, such as BN (Ioffe and Szegedy 2015), WN (Salimans and Kingma 2016; Gitman and Ginsburg 2017), WS (Qiao et al. 2019), etc. These methods can reduce the Lipschitz constant of the loss function and smooth the optimization landscape. Apart from applying to samples and weight vectors, GC (Yong et al. 2020a) computes the mean of gradients and centralizes the gradients to have zero mean instead of operating standardization on gradients, which also have good Lipschitz property, smooth the DNN training and improves the generalization performance with a strong restraint by projecting the gradient on a hyperplane. Apart from the statistics operation on gradients, how about applying adaptive factors to all gradients in each iteration? Based on an assumption we propose that when gradient magnitudes in all directions remain consistent, the training process will be more smooth and stable. Hence, we compute the factor by the ratio of each gradient to the sum of gradients in a neural network layer. Then, each gradient subtracts the product of itself and the corresponding factor to replace rigid traditional gradient clipping as a new regularization method. It can also be viewed as an adaptive learning rate scaling method.

3.2 Definitions and Preliminaries

There are some notations to be defined. We consider the gradients of the weight matrix in convolutional layers and fully connected layers. For convolutional layers, we denote weight matrix (kernel) $\mathbf{W}_C \in \mathbb{R}^{C_{in} \times C_{out} \times K \times K}$, C_{in} is the number of input channels, C_{out} is the number of output channels, $K \times K$ is the size of convolutional kernel. For fully connected layers, we denote weight matrix $\mathbf{W}_F \in \mathbb{R}^{C_{in} \times C_{out}}$, C_{in} is the number of input channels, C_{out} is the number of output channels. For simplicity, we denote the weight matrix $\mathbf{W} \in \mathbb{R}^{M \times N}$ in unified format. In addition, $\mathbf{w}_{i,j}$ is the element in i -th row and j -th column in \mathbf{W} ($i = 1, 2, \dots, M$; $j = 1, 2, \dots, N$). Denote \mathbf{W} the weight matrix and \mathcal{L} the objective function. $\nabla_{\mathbf{w}} \mathcal{L}$ and $\nabla_{\mathbf{w}_{i,j}} \mathcal{L}$ denote the gradient of \mathcal{L} w.r.t. the weight matrix \mathbf{W} and weight $\mathbf{w}_{i,j}$. $|\nabla_{\mathbf{w}} \mathcal{L}|$ and $|\nabla_{\mathbf{w}_{i,j}} \mathcal{L}|$ denote the absolute value of $\nabla_{\mathbf{w}} \mathcal{L}$ and $\nabla_{\mathbf{w}_{i,j}} \mathcal{L}$. $\sum \nabla_{\mathbf{w}_{i,j}} \mathcal{L}$ is the sum of $\nabla_{\mathbf{w}_{i,j}} \mathcal{L}$ in all dimensions.

3.3 AGR Formulation

For the fully connected layer and convolutional layer, suppose the gradient of weight $\mathbf{w}_{i,j}$ is $\nabla_{\mathbf{w}_{i,j}} \mathcal{L}$ ($i = 1, 2, \dots, M$; $j = 1, 2, \dots, N$). Denote the AGR operator Ψ , defined as below:

$$\Psi(\nabla_{\mathbf{w}_{i,j}} \mathcal{L}) = \nabla_{\mathbf{w}_{i,j}} \mathcal{L} - \alpha_{i,j} \nabla_{\mathbf{w}_{i,j}} \mathcal{L} \quad (1)$$

$$\alpha_{i,j} = \frac{|\nabla_{\mathbf{w}_{i,j}} \mathcal{L}|}{\sum |\nabla_{\mathbf{w}_{i,j}} \mathcal{L}|} \quad (2)$$

The simple calculation $\alpha_{i,j}$ is the ratio of the gradient absolute value to the sum of the gradient absolute values of the gradient matrix in all dimensions. Hence, the weight update in each iteration with AGR is below:

$$\mathbf{w}^{t+1} = \mathbf{w}^t - \eta \Psi(\nabla_{\mathbf{w}_{i,j}} \mathcal{L}) \quad (3)$$

3.4 Apply AGR to AdamW/Adan Optimizers

It is convenient and compact to embed AGR into AdamW (Loshchilov and Hutter 2017) and Adan (Xie et al. 2022) with just two lines of code. In Algorithm 1 and Algorithm 2, we update the weight by replacing $\nabla_{\mathbf{w}_{i,j}} \mathcal{L}$ with $\Psi(\nabla_{\mathbf{w}_{i,j}} \mathcal{L})$ to implement AGR in AdamW and Adan, respectively. We also find no additional computational cost and training time across networks. Notably, we only apply the AGR to the gradients and the first-order momentum instead of the second-order momentum because we expect to reduce the learning rate and gradient consistently when the gradient is large.

4. AGR Properties

In the following experimental results, we will see how AGR embedded into Adan or AdamW improves the generalization performance and training speed across multiple neural networks. In this section, let us give a detailed theoretical analysis of why it works well.

4.1 Adaptive Gradient Regularization

Smooth the loss landscape It has been proved that batch normalization(BN) (Ioffe and Szegedy 2015) and weight standardization(WS) (Qiao et al. 2019) can smooth the

Algorithm 1: Adan with AGR

Input: initialization θ_0 , step size η , momentum $(\beta_1, \beta_2, \beta_3) \in [0, 1]^3$, stable parameter $\epsilon > 0$, weight decay $\lambda_k > 0$, restart condition. $\mathbf{m}_0 = \mathbf{g}_0$, $\mathbf{v}_0 = 0$, $\mathbf{v}_1 = \mathbf{g}_1 - \mathbf{g}_0$, $\mathbf{n}_0 = \mathbf{g}_0^2$.

Output: some average of $\{\theta_k\}_{k=1}^K$

```

1: while  $k < K$  do
2:   calculate the stochastic gradient  $\mathbf{g}_k$  at  $\theta_k$ ;
    $\overline{\mathbf{g}_k} = \Psi(\mathbf{g}_k)$ ;
    $\mathbf{m}_k = (1 - \beta_1)\mathbf{m}_{k-1} + \beta_1 \overline{\mathbf{g}_k}$ ;
    $\mathbf{v}_k = (1 - \beta_2)\mathbf{v}_{k-1} + \beta_2(\overline{\mathbf{g}_k} - \mathbf{g}_{k-1})$ ;
    $\mathbf{n}_k = (1 - \beta_3)\mathbf{n}_{k-1} + \beta_3[\mathbf{g}_k + (1 - \beta_2)(\mathbf{g}_k - \mathbf{g}_{k-1})]^2$ ;
    $\eta_k = \eta / (\sqrt{\mathbf{n}_k} + \epsilon)$ ;
    $\theta_{k+1} = (1 + \lambda_k \eta)^{-1} [\theta_k - \eta_k \circ (\mathbf{m}_k + (1 - \beta_2)\mathbf{v}_k)]$ ;
3: if restart condition holds then
4:   estimate stochastic gradient  $\mathbf{g}_0$  at  $\theta_{k+1}$ ;
   set  $k = 1$  and update  $\theta_1$  by Line 6;
5: end if
6: end while

```

Algorithm 2: AdamW with AGR

Input: given $\alpha = 0.001$, $\beta_1 = 0.9$, $\beta_2 = 0.999$, $\epsilon = 10^{-8}$, $\lambda \in \mathbb{R}$.

Parameters: initialize time step $t \leftarrow 0$, parameter vector $\theta_{t=0} \in \mathbb{R}^n$, first moment vector $\mathbf{m}_{t=0} \leftarrow \mathbf{0}$, second moment vector $\mathbf{v}_{t=0} \leftarrow \mathbf{0}$, schedule multiplier $\eta_{t=0} \in \mathbb{R}$

Output: optimized parameters θ_t

```

1: repeat
2:    $t \leftarrow t + 1$ ;
    $\nabla f_t(\theta_{t-1}) \leftarrow \text{SelectBatch}(\theta_{t-1})$ ;
    $\mathbf{g}_t \leftarrow \nabla f_t(\theta_{t-1}) + \lambda \theta_{t-1}$ ;
    $\overline{\mathbf{g}_t} = \Psi(\mathbf{g}_t)$ ;
    $\mathbf{m}_t \leftarrow \beta_1 \mathbf{m}_{t-1} + (1 - \beta_1) \overline{\mathbf{g}_t}$ ;
    $\mathbf{v}_t \leftarrow \beta_2 \mathbf{v}_{t-1} + (1 - \beta_2) \mathbf{g}_t^2$ ;
    $\hat{\mathbf{m}}_t \leftarrow \mathbf{m}_t / (1 - \beta_1^t)$ ;
    $\hat{\mathbf{v}}_t \leftarrow \mathbf{v}_t / (1 - \beta_2^t)$ ;
    $\eta_t \leftarrow \text{SetScheduleMultiplier}(t)$ 
    $\theta_t \leftarrow \theta_{t-1} - \eta_t (\alpha \hat{\mathbf{m}}_t / (\sqrt{\hat{\mathbf{v}}_t} + \epsilon) + \lambda \theta_{t-1})$ 
3: until stopping criterion is met

```

loss landscape during the training process by reducing the Lipschitz constants of the loss and its gradients. GC (Yong et al. 2020a) also performs a theory analysis that this method can make the gradient of weight and the Hessian matrix of weight more stable. Specifically, GC (Yong et al. 2020a) use the magnitude of $\|\nabla_{\mathbf{w}} \mathcal{L}\|_2$ and $\|\nabla_{\mathbf{w}}^2 \mathcal{L}\|_2$ to capture the Lipschitzness of loss and its gradient, respectively. BN and WS can smooth the loss landscape with operation on weight, providing better Lipschitz properties by indirectly constraining the loss function and its gradients. GC smooths the loss landscape by direct operation on gradients. We also use this mathematical property to give a theory analysis of the AGR method as below and obtain a similar conclusion.

Theorem 4.1 $\nabla_{\mathbf{w}} \mathcal{L}$ is the gradient of loss function \mathcal{L} w.r.t. weight \mathbf{w} , with the function $\Psi(\nabla_{\mathbf{w}} \mathcal{L})$ defined in Eq.(2), we can give the following conclusion about the loss function and its gradient:

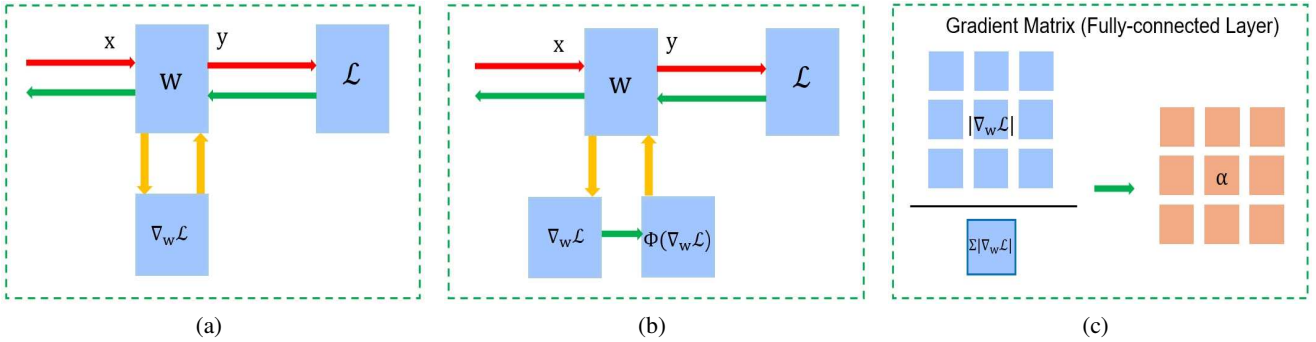


Figure 1: (a),(b) are sketches of how the AGR is embedded into the vanilla optimizer. \mathbf{W} is the weight tensor, \mathcal{L} is the loss function, $\nabla_w \mathcal{L}$ is the gradient of weight, and $\Psi(\nabla_w \mathcal{L})$ is the gradient with AGR method. (c) is the sketch of the AGR calculation, $|\nabla_w \mathcal{L}|$ is the absolute value of the gradient, $|\sum \nabla_w \mathcal{L}|$ is the sum of $|\nabla_w \mathcal{L}|$ w.r.t all dimensions. The black line represents the ratio, we can obtain the corresponding coefficient matrix.

$$\begin{cases} \|\Psi(\nabla_w \mathcal{L})\|_2 \leq \|\nabla_w \mathcal{L}\|_2, \\ \|\nabla_w \Psi(\nabla_w \mathcal{L})\|_2 \leq \|\nabla_w^2 \mathcal{L}\|_2, \end{cases} \quad (4)$$

The proof of theorem 4.1 is attached in the [Appendix](#). It shows that the loss \mathcal{L} and its gradient $\nabla_w \mathcal{L}$ are restrained with the AGR method. Like BN, WS, and GC, our method provides better Lipschitzness by implementing a dynamic regularization on the gradients.

4.2 Adaptive Learning Rate

Adjust learning rate depending on gradient During the weight iteration process, the learning rate and gradient contribute to the update direction and magnitude together (Cutkosky et al. 2023). The first-order momentum and second-order momentum are introduced to accelerate loss descending and scaling learning rate, respectively. In addition, the adaptive learning rate depends on the gradient magnitude. In other words, the learning rate in each iteration for a weight is integrated with its gradient. From this perspective, our AGR method also integrates an adaptive learning rate with a specific gradient.

Theorem 4.2 *AGR can adapt learning rate $\eta_{i,j}$ integrated with the gradient $\nabla_{w_{i,j}} \mathcal{L}$, their adaption tendency keep consistent.*

The proof of theorem 4.2 is attached in the [Appendix](#). From this perspective, we can understand that the operation on gradients and the learning rate are not separate. It is a better way to view why the AGR works well. Hence, we can expect faster training speed and better generalization performance due to the smoother loss landscape.

5. Experimental Result

We apply our AGR method to vision tasks and natural language processing (NLP) tasks. Vision tasks consist of image generation and classification. In the image generation task, we evaluate the AGR method to the representative SOTA backbone U-Net (Ronneberger et al. 2015) in the denoising diffusion probabilistic model (DDPM) (Ho et al. 2020). In the image classification task, we mainly investigate the ARG method under the conventional supervised setting, including CNN-type architectures: ResNets (He et al. 2016), VGG

(Iglovikov and Shvets 2018), ConvNext (Liu et al. 2022) and transformer-type architectures: ViT (Yin et al. 2022; Yuan et al. 2021) and Swin (Liu et al. 2021; Liang et al. 2021). In the NLP task, we evaluate the AGR method in ABERT. (Devlin et al. 2018; Lan et al. 2019)

We focus on applying ARG to the SoTA optimizer in the architectures mentioned above to evaluate their performance. For example, In the image classification task, the default/SoTA optimizer is AdamW (Loshchilov and Hutter 2017) in CNN-type architectures and ViTs. In the NLP task, the default/SoTA optimizer is LAMB and we set the optimizer as AdamW. Except for that, we also apply the AGR method to Adan (Xie et al. 2022) optimizer, which achieves better performance than AdamW in U-Net architecture under the image generation task. Restricted to the computational resource, we do not implement the ARG modification in all optimizers like SGD and Adam under all tasks. We also focus on AdamW because SGD and Adam achieve much worse accuracy than AdamW in image classification and generation tasks.

5.1 Experimental Setup

For evaluating and validating the AGR method generally and comprehensively, we conduct our experiments across image generation, image classification, and NLP tasks across multiple popular neural networks and open-source datasets. We arrange our experiments as follows:

- We first conduct an image generation task on the CIFAR10 dataset (Krizhevsky et al. 2010), which consists of 10 classes, and each class has 5000 images for training and 1000 for testing. The image resolution is 32×32 . In this task, we use the famous diffusion model paradigm: Denoising Diffusion Probabilistic Model (DDPM) with U-Net architecture as a solver for training and apply the AGR to the Adan optimizer. For comparison, we also conduct experiments with other popular optimizers.
- Next, we conduct a traditional image classification task on the CIFAR100 dataset (Lin et al. 2013), and Tiny-ImageNet (Le and Yang 2015) across multiple classical neural networks (VGG, ResNet, ViTs, ConvNext, etc.). Due to the restricted resources, we only train the tiny

Table 1: IS and its standard deviation(std) among different optimizers in DDPM on CIFAR10

IS↑	10	400	800	1200	1600	2000
ACProp	2.95 (0.03)	7.48 (0.07)	8.30 (0.07)	8.44 (0.09)	9.18 (0.16)	9.83 (0.17)
RMSprop	3.92 (0.04)	6.94 (0.07)	8.62 (0.14)	8.61 (0.05)	9.25 (0.12)	9.30 (0.06)
Adam	3.76 (0.04)	7.73 (0.13)	8.44 (0.11)	8.96 (0.16)	9.01 (0.09)	9.16 (0.13)
AdamW	3.99 (0.04)	7.84 (0.08)	8.91 (0.12)	9.02 (0.04)	9.11 (0.09)	9.18 (0.15)
Adan	4.31 (0.06)	8.14 (0.13)	8.85 (0.10)	9.18 (0.10)	9.19 (0.07)	9.22 (0.11)
Adan(AGR)	4.38(0.05)	8.32 (0.10)	8.86 (0.12)	9.18 (0.08)	9.26 (0.13)	9.34 (0.12)

Table 2: FID score on CIFAR10 dataset among optimizers

FID↓	10	400	800	1200	1600	2000
ACProp	304.03	40.06	28.42	12.32	10.12	9.57
RMSprop	313.19	54.67	23.56	10.35	8.40	8.10
Adam	229.30	55.12	21.91	10.45	10.27	9.27
AdamW	210.46	23.90	17.43	10.05	9.11	9.01
Adan	169.32	14.60	13.68	8.64	8.07	7.98
Adan(AGR)	161.65	13.48	12.75	8.08	7.85	7.44

version of ViTs and ConvNext. The CIFAR100 dataset consists of 100 classes, each with 500 images for training and 100 for testing. The image resolution is 32×32 . The Tiny-ImageNet consists of 200 classes, each with 500 images for training, 50 for validating, and 50 for testing. The image resolution is 64×64 . Due to the images in the test dataset not having class labels, we use the validation dataset for evaluation.

- Finally, we conduct language representation tasks on the WikiText-2 dataset (Radford et al. 2019). Due to the restricted resources, we train Albert (Lan et al. 2019), a lite version of Bert, for masked language model (MLM) and sentence order prediction (SOP) tasks.
- For better evaluation, each experiment is conducted four times, and then we calculate their mean as the final result.

If there is no additional note, we apply the AGR method to the fully connected layers and convolutional layers across all neural architectures in this work. For Adan and AdamW, we keep all default sets while using the LambdaLR learning rate scheduler if comparison experiments are not conducted on the hyperparameters. There is no integrated and additional operation on the optimizers except for the simple two codes representing the AGR method. All experiments are conducted on NVIDIA A40 with Pytorch framework as a 2.0 version.

5.2 Generative Model: DDPM

In this section, we present the results of DDPM training on the CIFAR10 dataset with different optimizers. We evaluate the performance with FID and IS scores, respectively., we also calculate the standard deviation of the IS score of generating 50000 images. For each experiment, we train DDPM with 2000 epochs and a batch size of 128. To save time, we introduce the denoising diffusion implicit model (DDIM) (Song et al. 2020) with steps as 100 for acceleration generation in each evaluation. As shown in Table 1 and Table 2, the Adan optimizer achieves the best performance among the popular optimizers, which also certifies its efficiency in the image generation task. Notably, Adan(AGR) improves

performance with a lower FID score and higher IS score. It shows that the AGR method improves the performance of U-Net architecture in predicting noise, which verifies that AGR is an efficient optimizer development technique for image generation. We also consider transferring this method to other diffusion model paradigms in future work to verify its more general performance. We need to stress that we focus on the comparison of performance after embedding the AGR method under the same setting. Hence, we don’t pay attention to the hyperparameter tuning for more accuracy.

5.3 Supervised Classification on TinyImageNet and CIFAR100

In this section, we conduct the traditional image classification task on the CIFAR100 and Tiny-ImageNet datasets. We train VGG11, ResNet-18, ResNet-50, and ResNet-101 architectures on the CIFAR100 dataset and train ConvNext and ViTs architectures on the Tiny-ImageNet dataset. We focus on applying the AGR on the AdamW optimizer. On the CIFAR100 dataset, each experiment is conducted in 200 epochs on 2 GPUs with batch size 64 per GPU. On the Tiny-ImageNet dataset, each experiment is conducted in 300 epochs on 2 GPUs with batch size 128 per GPU.

5.3.1 Results on CIFAR100

In this section, we evaluate the AGR method with some classical CNN- architectures on the CIFAR100 dataset, and we can see that the Top-1 accuracy can be improved to different degrees. As Figure 2 shows, the training loss dives deeper with the AGR method, and the test accuracy is improved and more smooth, which shows that the AGR method can stabilize the training process and improve the general performance in the ResNet18 backbone. We also apply the AGR to AdamW on other popular backbones such as ResNet50 and ResNet101. As Figure 3 shows, the training loss landscape of VGG11 with the AGR method is smoother with higher performance. Hence, it achieves better accuracy in the test datasets in a smoother way, which verifies that the AGR can accelerate the training process and improve the generalization ability of AdamW in the VGG11 backbone. We also present the evaluation result of the AGR on the ResNet18 backbone. As Table 3 shows, the AGR method could improve the performance of around 1% of AdamW on them.

5.3.2 Results on Tiny-ImageNet

In this section, we evaluate the AGR method on transformer architectures and ConvNext on the Tiny-imageNet dataset. For a more comprehensive comparison, we apply

Table 3: Top-1 ACC.(%) of ConvNext and Swin on Tiny-ImageNet under the official settings

Epoch	ConvNext Tiny			ConvNext Tiny			Swin Tiny			Swin Small		
	100	200	300	100	200	300	100	200	300	100	200	300
AdamW	64.78	67.47	68.47	65.92	67.81	70.02	64.79	69.85	72.01	65.43	70.49	72.12
AdamW(AGR)	64.98	67.71	69.03	66.12	68.90	70.54	65.17	70.16	72.21	66.02	70.69	72.39

Table 4: Top-1 ACC.(%) of ViTs on Tiny-ImageNet under the official setting

Epoch	TinyViT-5M			TinyViT-11M			TinyViT-21M		
	100	200	300	100	200	300	100	200	300
AdamW	61.80	68.14	69.50	63.91	70.25	71.39	65.06	71.38	72.50
AdamW(AGR)	62.96	68.75	69.83	65.71	72.45	73.02	66.13	71.94	72.96

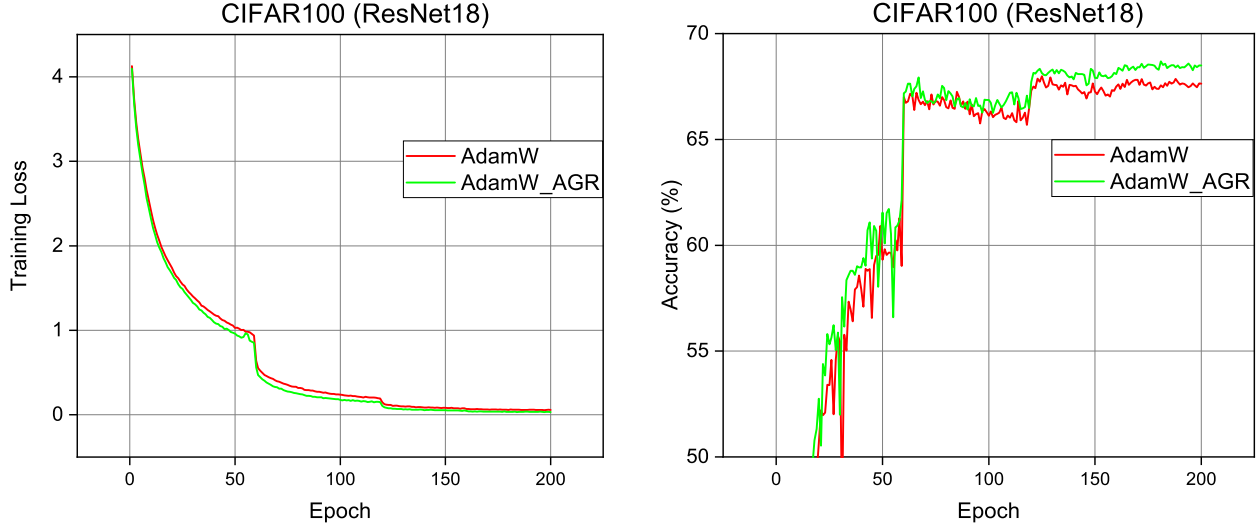


Figure 2: Training loss test accuracy (c,b) of ResNet18 structures in Tiny-Imagenet, AGR represents AGR is embedded into AdamW optimizer.

the AGR to multiple variants of TinyViT, Swin, and ConvNext. Specifically, there are three variants of TinyViT with 5M, 11M, and 21M parameters. There are also tiny versions of ConvNext and Swin, respectively. As Figure 3 shows, the AGR method could reduce the training loss and improve the test accuracy mostly through the entire training process. The test accuracy of Swin-Tiny is improved more in the later epochs of training, which also improves the generalization capability and accelerates the training process. As Table 3 shows, the AGR method can improve the performance $>0.5\%$ in general on ConvNext and Swin backbones. As Table 4 shows, the test accuracy in TinyViT variants is improved by 1.7% at most. Similar to the multiple ResNet variants, TinyViT with more parameters cannot also excavate more pattern information due to the limited training images which achieves a little higher accuracy than TinyViT with fewer parameters. Hence, the AGR method can be embedded into multiple neural networks in the transformer architecture.

5.4 Language Representations: ALBERT

In this section, we evaluate the AGR method on the natural language representation tasks with the lite version of

BERT: Abert. The language representation tasks consist of masked language model (MLM) and sentence order prediction (SOP). We evaluate the performance of the WikiText-2 dataset on a single GPU. Each experiment is conducted in 25 epochs with batch size 16. In this section, we also evaluate the AGR method across different weight decay in AdamW. As Table 6 shows, the AGR method can improve the SOP accuracy across different weight decay, and we also see the importance of weight decay in the model training process.

5.5 Ablation Study

Through extensive experiments, we found that the AGR method cannot improve the training performance during the entire process. According to our theoretical analysis, the gradient and learning rate will be reduced adaptively based on the current gradient magnitude. The learning rate will decrease more when the gradient magnitude is larger. However, the learning rate needs to be larger in the later training epochs. Hence, the performance will be better when suspending the AGR method after a period of training. In this section, we conduct experiments on image classification tasks with the TinyViT-11M backbone and evaluate the influence of the AGR running epochs. As Table 7 shows,

Table 5: Top-1 ACC.(%) of ResNet and VGG11 on Tiny-ImageNet under the official settings

Epoch	VGG11			ResNet-18			ResNet-50			ResNet-101		
	50	150	200	50	150	200	50	150	200	50	150	200
AdamW	61.95	65.09	65.40	59.31	67.26	67.64	61.26	68.19	68.80	61.47	68.61	69.33
AdamW(AGR)	61.45	65.48	65.73	61.54	67.91	68.50	63.08	68.22	69.38	64.11	68.92	69.73

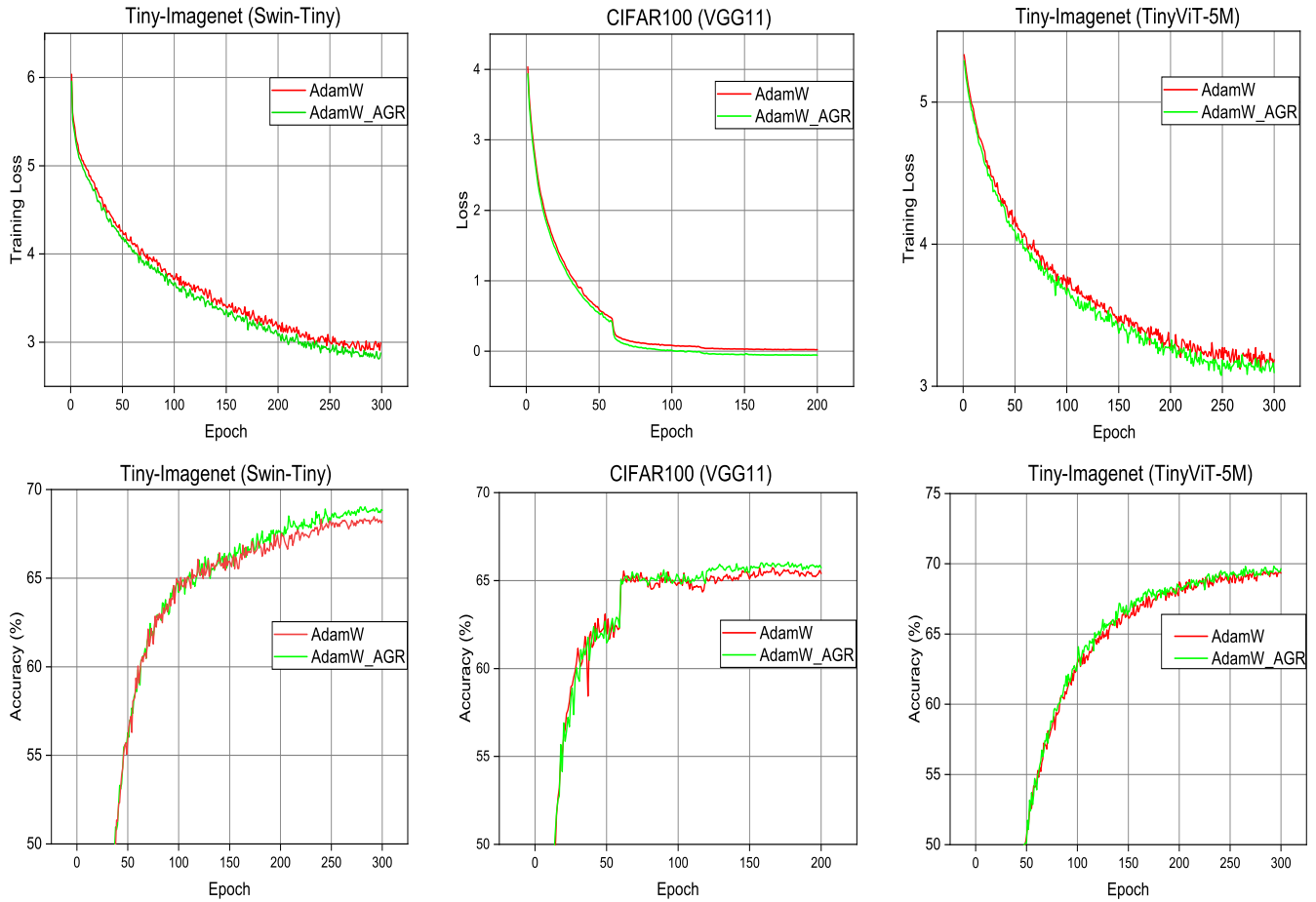


Figure 3: Training loss (a,b) and test accuracy (c,b) of TinyViT and ResNet18 structures in Tiny-Imagenet, AGR is embedded into AdamW optimizer.

Table 6: SOP ACC.(%) of Albert on Wiki-Text2 dataset

Weight decay	0	2e-4	5e-4	1e-3	1e-2
AdamW	80.02	82.14	83.01	82.94	82.73
AdamW(AGR)	80.55	84.19	84.47	83.21	83.06

Table 7: Top-1 ACC.(%) of TinyViT-11M on Tiny-ImageNet

Epochs	0	100	150	200	250	300
AdamW(AGR)	71.39	71.57	72.88	72.92	73.58	73.02

when running the AGR method with 250 epochs instead of entire epochs, we can achieve higher accuracy. This verifies our analysis that the learning rate in the later training epochs should be kept larger.

6. Conclusions

We proposed a new optimization technique that normalizes the gradient vector as its coefficient vector based on the gra-

dient magnitude and subtracts the dot of the gradient vector and its coefficient vector from the vanilla gradient vector. Hence, the gradient can be regularized in an adaptive way named adaptive gradient regularization (AGR). From theory analysis, we show that the AGR can improve the Lipschitzness of the loss function. Then, extensive experiments on image generation, image classification, and natural language processing show that the AGR can stabilize the training process and accelerate the training with better generalization.

References

Assran, M. and Rabbat, M. G. (2020). On the convergence of nesterov's accelerated gradient method in stochastic settings. *ArXiv*, abs/2002.12414.

Ba, J. L., Kiros, J. R., and Hinton, G. E. (2016). Layer normalization. *arXiv preprint arXiv:1607.06450*.

Bergstra, J., Yamins, D., and Cox, D. D. (2013). Making a science of model search: hyperparameter optimization in hundreds of dimensions for vision architectures. In *Proceedings of the 30th International Conference on International Conference on Machine Learning - Volume 28*, ICML'13, page I–115–I–123. JMLR.org.

Botev, A., Lever, G., and Barber, D. (2017). Nesterov’s accelerated gradient and momentum as approximations to regularised update descent. In *2017 International Joint Conference on Neural Networks (IJCNN)*, pages 1899–1903.

Bottou, L. (2012). Stochastic gradient descent tricks. In *Neural Networks*.

Chen, J., Zhou, D., Tang, Y., Yang, Z., Cao, Y., and Gu, Q. (2018a). Closing the generalization gap of adaptive gradient methods in training deep neural networks. *arXiv preprint arXiv:1806.06763*.

Chen, X., Wu, S. Z., and Hong, M. (2020). Understanding gradient clipping in private sgd: A geometric perspective. *Advances in Neural Information Processing Systems*, 33:13773–13782.

Chen, Z., Badrinarayanan, V., Lee, C.-Y., and Rabinovich, A. (2018b). Gradnorm: Gradient normalization for adaptive loss balancing in deep multitask networks. In *International conference on machine learning*, pages 794–803. PMLR.

Chmiel, B., Ben-Uri, L., Shkolnik, M., Hoffer, E., Banner, R., and Soudry, D. (2020). Neural gradients are near-lognormal: improved quantized and sparse training. *arXiv preprint arXiv:2006.08173*.

Cutkosky, A., Defazio, A., and Mehta, H. (2023). Mechanic: A learning rate tuner. *Neural Information Processing Systems*.

Devlin, J., Chang, M.-W., Lee, K., and Toutanova, K. (2018). Bert: Pre-training of deep bidirectional transformers for language understanding. *arXiv preprint arXiv:1810.04805*.

Duchi, J., Hazan, E., and Singer, Y. (2011). Adaptive subgradient methods for online learning and stochastic optimization. *J. Mach. Learn. Res.*, 12(null):2121–2159.

Ghadimi, S. and Lan, G. (2013). Stochastic first- and zeroth-order methods for nonconvex stochastic programming. *SIAM Journal on Optimization*, 23(4):2341–2368.

Gitman, I. and Ginsburg, B. (2017). Comparison of batch normalization and weight normalization algorithms for the large-scale image classification. *arXiv preprint arXiv:1709.08145*.

Goldberg, Y. (2016). A primer on neural network models for natural language processing. *Journal of Artificial Intelligence Research*, 57:345–420.

Guo, B., Liu, Y., and Zhang, C. (2021). A partition based gradient compression algorithm for distributed training in aiot. *Sensors*, 21(6):1943.

Guo, M.-H., Xu, T.-X., Liu, J.-J., Liu, Z.-N., Jiang, P.-T., Mu, T.-J., Zhang, S.-H., Martin, R. R., Cheng, M.-M., and Hu, S.-M. (2022). Attention mechanisms in computer vision: A survey. *Computational visual media*, 8(3):331–368.

He, K., Zhang, X., Ren, S., and Sun, J. (2016). Identity mappings in deep residual networks. In *Computer Vision–ECCV 2016: 14th European Conference, Amsterdam, The Netherlands, October 11–14, 2016, Proceedings, Part IV 14*, pages 630–645. Springer.

Ho, J., Jain, A., and Abbeel, P. (2020). Denoising diffusion probabilistic models. *Advances in neural information processing systems*, 33:6840–6851.

Iglovikov, V. and Shvets, A. (2018). Ternausnet: U-net with vgg11 encoder pre-trained on imagenet for image segmentation. *arXiv preprint arXiv:1801.05746*.

Ioffe, S. and Szegedy, C. (2015). Batch normalization: Accelerating deep network training by reducing internal covariate shift. In *International conference on machine learning*, pages 448–456. pmlr.

Kingma, D. P. and Ba, J. (2014). Adam: A method for stochastic optimization. *CoRR*, abs/1412.6980.

Krizhevsky, A., Hinton, G., et al. (2010). Convolutional deep belief networks on cifar-10. *Unpublished manuscript*, 40(7):1–9.

Lan, Z., Chen, M., Goodman, S., Gimpel, K., Sharma, P., and Soricut, R. (2019). Albert: A lite bert for self-supervised learning of language representations. *arXiv preprint arXiv:1909.11942*.

Le, Y. and Yang, X. (2015). Tiny imagenet visual recognition challenge. *CS 231N*, 7(7):3.

Liang, J., Cao, J., Sun, G., Zhang, K., Van Gool, L., and Timofte, R. (2021). Swinir: Image restoration using swin transformer. In *Proceedings of the IEEE/CVF international conference on computer vision*, pages 1833–1844.

Lin, M., Chen, Q., and Yan, S. (2013). Network in network. *arXiv preprint arXiv:1312.4400*.

Liu, W., Wang, Z., Liu, X., Zeng, N., Liu, Y., and Alsaadi, F. E. (2017). A survey of deep neural network architectures and their applications. *Neurocomputing*, 234:11–26.

Liu, Z., Lin, Y., Cao, Y., Hu, H., Wei, Y., Zhang, Z., Lin, S., and Guo, B. (2021). Swin transformer: Hierarchical vision transformer using shifted windows. In *Proceedings of the IEEE/CVF international conference on computer vision*, pages 10012–10022.

Liu, Z., Mao, H., Wu, C.-Y., Feichtenhofer, C., Darrell, T., and Xie, S. (2022). A convnet for the 2020s. In *Proceedings of the IEEE/CVF conference on computer vision and pattern recognition*, pages 11976–11986.

Loshchilov, I. and Hutter, F. (2017). Decoupled weight decay regularization. In *International Conference on Learning Representations*.

Menon, A. K., Rawat, A. S., Reddi, S. J., and Kumar, S. (2019). Can gradient clipping mitigate label noise? In *International Conference on Learning Representations*.

Nesterov, Y. (2014). Introductory lectures on convex optimization - a basic course. In *Applied Optimization*.

Qian, N. (1999). On the momentum term in gradient descent learning algorithms. *Neural Networks*, 12(1):145–151.

Qiao, S., Wang, H., Liu, C., Shen, W., and Yuille, A. L. (2019). Weight standardization. *ArXiv*, abs/1903.10520.

Radford, A., Wu, J., Child, R., Luan, D., Amodei, D., Sutskever, I., et al. (2019). Language models are unsupervised multitask learners. *OpenAI blog*, 1(8):9.

Robinson, A. L. (1980). New ways to make microcircuits smaller. *Science*, 208(4447):1019–1022.

Ronneberger, O., Fischer, P., and Brox, T. (2015). U-net: Convolutional networks for biomedical image segmentation. In Navab, N., Hornegger, J., Wells, W. M., and Frangi, A. F., editors, *Medical Image Computing and Computer-Assisted Intervention – MICCAI 2015*, pages 234–241, Cham. Springer International Publishing.

Ruder, S. (2016). An overview of gradient descent optimization algorithms. *arXiv preprint arXiv:1609.04747*.

Salimans, T. and Kingma, D. P. (2016). Weight normalization: A simple reparameterization to accelerate training of deep neural networks. *Advances in neural information processing systems*, 29.

Song, J., Meng, C., and Ermon, S. (2020). Denoising diffusion implicit models. *arXiv preprint arXiv:2010.02502*.

Tran, T. H., Scheinberg, K., and Nguyen, L. M. (2022). Nesterov accelerated shuffling gradient method for convex optimization. In *International Conference on Machine Learning*, pages 21703–21732. PMLR.

Ulyanov, D., Vedaldi, A., and Lempitsky, V. S. (2016). Instance normalization: The missing ingredient for fast stylization. *ArXiv*, abs/1607.08022.

Wiedemann, S., Mehari, T., Kepp, K., and Samek, W. (2020). Dithered backprop: A sparse and quantized backpropagation algorithm for more efficient deep neural network training. *2020 IEEE/CVF Conference on Computer Vision and Pattern Recognition Workshops (CVPRW)*, pages 3096–3104.

Wu, Y. and He, K. (2018). Group normalization. In *Proceedings of the European conference on computer vision (ECCV)*, pages 3–19.

Wu, Y.-L., Shuai, H.-H., Tam, Z.-R., and Chiu, H.-Y. (2021). Gradient normalization for generative adversarial networks. In *Proceedings of the IEEE/CVF international conference on computer vision*, pages 6373–6382.

Xie, X., Zhou, P., Li, H., Lin, Z., and Yan, S. (2022). Adan: Adaptive nesterov momentum algorithm for faster optimizing deep models. *arXiv preprint arXiv:2208.06677*.

Yang, L. and Shami, A. (2020). On hyperparameter optimization of machine learning algorithms: Theory and practice. *ArXiv*, abs/2007.15745.

Yin, H., Vahdat, A., Alvarez, J. M., Mallya, A., Kautz, J., and Molchanov, P. (2022). A-vit: Adaptive tokens for efficient vision transformer. In *Proceedings of the IEEE/CVF conference on computer vision and pattern recognition*, pages 10809–10818.

Yong, H., Huang, J., Hua, X., and Zhang, L. (2020a). Gradient centralization: A new optimization technique for deep neural networks. In *Computer Vision–ECCV 2020: 16th European Conference, Glasgow, UK, August 23–28, 2020, Proceedings, Part I 16*, pages 635–652. Springer.

Yong, H., Huang, J., Hua, X., and Zhang, L. (2020b). Gradient centralization: A new optimization technique for deep neural networks. In *Computer Vision–ECCV 2020: 16th European Conference, Glasgow, UK, August 23–28, 2020, Proceedings, Part I 16*, pages 635–652. Springer.

Yu, F., Seff, A., Zhang, Y., Song, S., Funkhouser, T., and Xiao, J. (2015). Lsun: Construction of a large-scale image dataset using deep learning with humans in the loop. *arXiv preprint arXiv:1506.03365*.

Yuan, L., Chen, Y., Wang, T., Yu, W., Shi, Y., Jiang, Z.-H., Tay, F. E., Feng, J., and Yan, S. (2021). Tokens-to-token vit: Training vision transformers from scratch on imagenet. In *Proceedings of the IEEE/CVF international conference on computer vision*, pages 558–567.

Zhang, J., He, T., Sra, S., and Jadbabaie, A. (2019a). Why gradient clipping accelerates training: A theoretical justification for adaptivity. *arXiv: Optimization and Control*.

Zhang, S., Yao, L., Sun, A., and Tay, Y. (2019b). Deep learning based recommender system: A survey and new perspectives. *ACM Comput. Surv.*, 52(1).

Zhuang, J., Ding, Y., Tang, T., Dvornek, N., Tatikonda, S., and Duncan, J. (2021). Momentum centering and asynchronous update for adaptive gradient methods. *Advances in Neural Information Processing Systems*, 34.

Zou, F., Shen, L., Jie, Z., Zhang, W., and Liu, W. (2019). A sufficient condition for convergences of adam and rmsprop. In *Proceedings of the IEEE/CVF Conference on computer vision and pattern recognition*, pages 11127–11135.

Appendix

A1. Theorem 4.1 Proof

Proof: For weight $w_{i,j}$ in weight vectors and definition in eq(1) and eq(2), we have:

$$\|\Psi(\nabla_{\mathbf{w}_{i,j}} \mathcal{L})\|_2^2 = \|\nabla_{\mathbf{w}_{i,j}} \mathcal{L}\|_2^2 (1 - \frac{|\nabla_{\mathbf{w}_{i,j}} \mathcal{L}|}{\sum |\nabla_{\mathbf{w}_{i,j}} \mathcal{L}|})^2 \leq \|\nabla_{\mathbf{w}_{i,j}} \mathcal{L}\|_2^2 \quad (5)$$

$$\nabla_{\mathbf{w}_{i,j}} \Psi(\nabla_{\mathbf{w}_{i,j}} \mathcal{L}) = \nabla_{\mathbf{w}_{i,j}}^2 \mathcal{L} (1 - \frac{|\nabla_{\mathbf{w}_{i,j}} \mathcal{L}|}{\sum |\nabla_{\mathbf{w}_{i,j}} \mathcal{L}|})^2 + \nabla_{\mathbf{w}_{i,j}} \mathcal{L} \nabla_{\mathbf{w}_{i,j}} (1 - \frac{|\nabla_{\mathbf{w}_{i,j}} \mathcal{L}|}{\sum |\nabla_{\mathbf{w}_{i,j}} \mathcal{L}|}) \quad (6)$$

Next, we need to discuss about two cases with $\nabla_{\mathbf{w}_{i,j}} \mathcal{L} < 0$ and $\nabla_{\mathbf{w}_{i,j}} \mathcal{L} \geq 0$
when $\nabla_{\mathbf{w}_{i,j}} \mathcal{L} \geq 0$:

$$\begin{aligned} \nabla_{\mathbf{w}_{i,j}} (1 - \frac{|\nabla_{\mathbf{w}_{i,j}} \mathcal{L}|}{\sum |\nabla_{\mathbf{w}_{i,j}} \mathcal{L}|}) &= -\nabla_{\mathbf{w}_{i,j}} \frac{\nabla_{\mathbf{w}_{i,j}} \mathcal{L}}{\sum |\nabla_{\mathbf{w}_{i,j}} \mathcal{L}|} \\ &= -\frac{\nabla_{\mathbf{w}_{i,j}}^2 \mathcal{L} \sum |\nabla_{\mathbf{w}_{i,j}} \mathcal{L}| - \nabla_{\mathbf{w}_{i,j}} \mathcal{L} \nabla_{\mathbf{w}_{i,j}} \sum |\nabla_{\mathbf{w}_{i,j}} \mathcal{L}|}{(\sum |\nabla_{\mathbf{w}_{i,j}} \mathcal{L}|)^2} \\ &= -\frac{\nabla_{\mathbf{w}_{i,j}}^2 \mathcal{L} \sum |\nabla_{\mathbf{w}_{i,j}} \mathcal{L}| - \nabla_{\mathbf{w}_{i,j}} \mathcal{L} \nabla_{\mathbf{w}_{i,j}}^2 \mathcal{L}}{(\sum |\nabla_{\mathbf{w}_{i,j}} \mathcal{L}|)^2} \end{aligned} \quad (7)$$

Combined with eq(6), we have:

$$\begin{aligned} \nabla_{\mathbf{w}_{i,j}} \Psi(\nabla_{\mathbf{w}_{i,j}} \mathcal{L}) &= \nabla_{\mathbf{w}_{i,j}}^2 \mathcal{L} (1 - \frac{|\nabla_{\mathbf{w}_{i,j}} \mathcal{L}|}{\sum |\nabla_{\mathbf{w}_{i,j}} \mathcal{L}|})^2 + \frac{\nabla_{\mathbf{w}_{i,j}}^2 \mathcal{L} \sum |\nabla_{\mathbf{w}_{i,j}} \mathcal{L}| + \nabla_{\mathbf{w}_{i,j}} \mathcal{L} \nabla_{\mathbf{w}_{i,j}}^2 \mathcal{L}}{(\sum |\nabla_{\mathbf{w}_{i,j}} \mathcal{L}|)^2} \\ &= \nabla_{\mathbf{w}_{i,j}}^2 \mathcal{L} \frac{(\sum |\nabla_{\mathbf{w}_{i,j}} \mathcal{L}|)^2 - 2 \nabla_{\mathbf{w}_{i,j}} \mathcal{L} \sum |\nabla_{\mathbf{w}_{i,j}} \mathcal{L}| + (\nabla_{\mathbf{w}_{i,j}} \mathcal{L})^2}{(\sum |\nabla_{\mathbf{w}_{i,j}} \mathcal{L}|)^2} \\ &= \nabla_{\mathbf{w}_{i,j}}^2 \mathcal{L} \frac{(\sum |\nabla_{\mathbf{w}_{i,j}} \mathcal{L}| - \nabla_{\mathbf{w}_{i,j}} \mathcal{L})^2}{(\sum |\nabla_{\mathbf{w}_{i,j}} \mathcal{L}|)^2} \\ &\leq \nabla_{\mathbf{w}_{i,j}}^2 \mathcal{L} \end{aligned} \quad (8)$$

when $\nabla_{\mathbf{w}_{i,j}} \mathcal{L} < 0$:

$$\begin{aligned} \nabla_{\mathbf{w}_{i,j}} (1 - \frac{|\nabla_{\mathbf{w}_{i,j}} \mathcal{L}|}{\sum |\nabla_{\mathbf{w}_{i,j}} \mathcal{L}|}) &= \nabla_{\mathbf{w}_{i,j}} \frac{\nabla_{\mathbf{w}_{i,j}} \mathcal{L}}{\sum |\nabla_{\mathbf{w}_{i,j}} \mathcal{L}|} \\ &= \frac{\nabla_{\mathbf{w}_{i,j}}^2 \mathcal{L} \sum |\nabla_{\mathbf{w}_{i,j}} \mathcal{L}| - \nabla_{\mathbf{w}_{i,j}} \mathcal{L} \nabla_{\mathbf{w}_{i,j}} \sum |\nabla_{\mathbf{w}_{i,j}} \mathcal{L}|}{(\sum |\nabla_{\mathbf{w}_{i,j}} \mathcal{L}|)^2} \\ &= \frac{\nabla_{\mathbf{w}_{i,j}}^2 \mathcal{L} \sum |\nabla_{\mathbf{w}_{i,j}} \mathcal{L}| + \nabla_{\mathbf{w}_{i,j}} \mathcal{L} \nabla_{\mathbf{w}_{i,j}}^2 \mathcal{L}}{(\sum |\nabla_{\mathbf{w}_{i,j}} \mathcal{L}|)^2} \end{aligned} \quad (9)$$

Combined with eq(6), we have:

$$\begin{aligned} \nabla_{\mathbf{w}_{i,j}} \Psi(\nabla_{\mathbf{w}_{i,j}} \mathcal{L}) &= \nabla_{\mathbf{w}_{i,j}}^2 \mathcal{L} (1 + \frac{\nabla_{\mathbf{w}_{i,j}} \mathcal{L}}{\sum |\nabla_{\mathbf{w}_{i,j}} \mathcal{L}|})^2 + \frac{\nabla_{\mathbf{w}_{i,j}}^2 \mathcal{L} \sum |\nabla_{\mathbf{w}_{i,j}} \mathcal{L}| + \nabla_{\mathbf{w}_{i,j}} \mathcal{L} \nabla_{\mathbf{w}_{i,j}}^2 \mathcal{L}}{(\sum |\nabla_{\mathbf{w}_{i,j}} \mathcal{L}|)^2} \\ &= \nabla_{\mathbf{w}_{i,j}}^2 \mathcal{L} \frac{(\sum |\nabla_{\mathbf{w}_{i,j}} \mathcal{L}|)^2 + 2 \nabla_{\mathbf{w}_{i,j}} \mathcal{L} \sum |\nabla_{\mathbf{w}_{i,j}} \mathcal{L}| + (\nabla_{\mathbf{w}_{i,j}} \mathcal{L})^2}{(\sum |\nabla_{\mathbf{w}_{i,j}} \mathcal{L}|)^2} \\ &= \nabla_{\mathbf{w}_{i,j}}^2 \mathcal{L} \frac{(\sum |\nabla_{\mathbf{w}_{i,j}} \mathcal{L}| + \nabla_{\mathbf{w}_{i,j}} \mathcal{L})^2}{(\sum |\nabla_{\mathbf{w}_{i,j}} \mathcal{L}|)^2} \\ &\leq \nabla_{\mathbf{w}_{i,j}}^2 \mathcal{L} \end{aligned} \quad (10)$$

In the optimization process, we need to find the optimal local minimum as the global minimum. Hence, the landscape of loss containing these local minima is convex. So we have:

$$\|\nabla_{\mathbf{w}_{i,j}} \Psi(\nabla_{\mathbf{w}_{i,j}} \mathcal{L})\|_2^2 \leq \|\nabla_{\mathbf{w}_{i,j}}^2 \mathcal{L}\|_2^2 \quad (11)$$

A2. Theorem 4.2 Proof

In this proof, we take optimizer AdamW with AGR to illustrate theorem 4.2 is certified. From the definition of momentum m_t in AdamW at t-st update for a specific weight, we can derive recursively:

$$m_t = \sum_{i=0}^{t-i} \beta_1^i (1 - \beta_1) (\Psi(\nabla_{\mathbf{w}_t} \mathcal{L}))_{t-i} \quad (12)$$

From the simplicity we don't apply ARG to the second-order momentum, we have the following weight update process:

$$\begin{aligned} w_{t+1} &= w_t - \eta_t m_t \\ &= w_t - \eta_t \sum_{i=0}^{t-i} \beta_1^i (1 - \beta_1) (\Psi(\nabla_{\mathbf{w}_t} \mathcal{L}))_{t-i} \\ &= w_t - \eta_t \sum_{i=0}^{t-i} \beta_1^i (1 - \beta_1) ((1 - \alpha_{t-i}) (\nabla_{\mathbf{w}_t} \mathcal{L}))_{t-i} \end{aligned} \quad (13)$$

Assume for each time $\alpha_{t-i} = \hat{\alpha}$ is the same for clearer certification, we have:

$$w_{t+1} = w_t - \eta_t \sqrt{(1 - \hat{\alpha}^t)} \sum_{i=0}^{t-i} \beta_1^i (1 - \beta_1) \sqrt{(1 - \hat{\alpha}^t)} (\nabla_{\mathbf{w}_t} \mathcal{L})_{t-i} \quad (14)$$

Through this perspective, we can see the same tendency in learning rate and gradient adaption with AGR.